Available online at www.sciencedirect.com
SCIENCE DIRECT
Polymer 47 (2006) 457–465
polymer
www.elsevier.com/locate/polymer

Synthesis and shape memory effects of Si–O–Si cross-linked hybrid polyurethanes

Jianwen Xu [a], Wenfang Shi [a,*], Wenmin Pang [b]

[a] State Key Laboratory of Fire Science and Department of Polymer Science and Engineering, University of Science and Technology of China, Hefei, Anhui 230026, People's Republic of China
[b] Structure Research Laboratory, University of Science and Technology of China, Hefei, Anhui 230026, People's Republic of China

Received 12 June 2005; received in revised form 20 September 2005; accepted 13 November 2005
Available online 29 November 2005

Abstract

A series of novel Si–O–Si cross-linked organic/inorganic hybrid polyurethanes (HYPUs) with shape memory effect were prepared from isophorone diisocyanate (IPDI), poly(ethylene oxide) (PEO), and a newly synthesized hybrid diol (HD) containing hydrolysable Si–OEt groups. After hydrolyzation and condensation of Si–OEt groups, the resulted films were characterized using wide-angle X-ray scattering (WAXS), differential scanning calorimetry (DSC), dynamic mechanical analysis (DMA) and shape recovery test to get the insight into the relationship between shape memory behaviors and polymeric structures. The glass transition temperatures (T_g) and storage modulus increased with Si–O–Si cross-linking increasing in the hybrid polyurethanes. The hybrid polyurethanes can recover to their original shapes almost completely in less than 40 s in atmosphere and in less than 10 s in water, respectively, when heated at 25 °C above T_g. The shape memory mechanism is coming from the freezing at low temperature and activation at high temperature of micro-Brownian movement of amorphous molecular chains since the temperature ranges at which the sharpest changes of recovered curvature happened are found to be around their glass transition range. The high ratio of storage modulus below and above T_g^{DMA} accounted for the temporary shape fixing at low temperature. The samples with more Si–O–Si cross-linking have higher storage modulus at high temperature, resulting in faster shape recovery speed but lower temporary shape fixing.

Keywords: Organic/inorganic; Polyurethane; Shape memory effect

1. Introduction

Stimuli-responsive materials, which can undergo large-scale shape or property changes in response to external stimulus such as stress, temperature, light or pH, have attracted great interest since they exhibit some 'intelligence' like the live. Thermo-responsive shape memory materials are one of the most widely studied stimuli-responsive materials [1], which can easily be deformed into a temporary shape when heated and to be fixed at the temporary shape after fast cooling down, then regain their original shape upon heating again. Thermo-responsive shape memory materials include shape memory alloys (SMA) and shape memory polymers (SMP), which have quite different shape memory mechanisms and mechanical properties changes. For SMA, the shape memory effect is based on a transition between austenitic phase at a higher temperature and martensitic phase at a lower temperature, and an increase of modulus with increasing temperature is usually observed. While the shape memory mechanism for SMP is based on recovery of entropy elasticity, and a reduction of the modulus normally follows raising temperature [2]. The shape memory effect was observed for the first time by Chang and Read in 1951 for a gold-cadmium alloy. In recent years, SMP have received greater interest than SMA because of their higher strain recovery levels, easier processing, lower density and lower cost.

A SMP usually consists of two phases: a fixing phase and a reversible phase. Chain entanglement, crystallization and cross-linking network can be used as a fixing phase for memorizing the original shape. Glass transition or melting of crystallite of molecular chains can be designed as a reversible phase, which would show high elasticity at high temperature for deformation from original shape to temporary shape [1,3–5]. Polyurethane-type shape memory polymers [6] are one of the most widely studied materials since its discovery by Mitsubishi

* Corresponding author. Tel.: +86 551 3606084; fax: +86 551 3606630.
E-mail address: wfshi@ustc.edu.cn (W. Shi).

0032-3861/$ - see front matter © 2005 Elsevier Ltd. All rights reserved.
doi:10.1016/j.polymer.2005.11.035

Heavy Industries Ltd in 1988. Due to the versatility of polyurethane synthesis, their macroscopic properties, such as mechanical properties and glass transition temperature (T_g), can be tailored by the variation of molecular parameters according to the requirement of specific applications. For example, segmented polyurethanes have a micro-phase separation structure due to the incompatibility of the hard segment and the soft segment, the characteristic temperatures of hard and soft segments can be designed to satisfy the demand for shape memory effect. Shape memory polyurethane have been found to be potential for a number of applications, such as auto choke, smart fabrics, deformable handle, medical device or biological micro-electromechanical systems (Bio-MEMS) and so on.

Most of researches have concentrated on physically cross-linked segmented polyurethanes, in which the physical cross-linking networks, i.e. the hard segment interaction networks with a higher T_g or melting temperature (T_m), are used to memorize the original shape and to retain the dimensional stability during deformation, while the entangled or crystallized molecular chains of soft segments with a lower T_g or T_m are used as a reversible phase, which become disentangled and deformable when heated above the T_g or T_m. However, it's normally observed in physically cross-linked shape memory polyurethane systems that the residual strain increases and the recovery strain decreases with increasing cycle and maximum strain, which is due to the plastic deformation of hard segment crystal or the flow of amorphous segments [7,8]. Much works have been done by several groups to reduce the relaxation process of polyurethane chains by introducing ionic groups [9] or mesogen units [10] into the hard segments, or by the cross-linking of hard segments and soft segments [11], or through the control of soft segment arrangement [12]. Recently, a chemically cross-linked biodegradable polyurethane with adjustable transition temperatures were prepared by Lendlein et al. from diisocyanates and co-polyesters with different functionality and segment length, which showed excellent fixation of temporary shape and recovery of original shape [13].

Another significant drawback of polyurethane shape memory materials is their low stiffness compared to metals and ceramics. In practical application environments, increasing stiffness of SMP is critical for enhancing recoverable stress levels during constrained recovery deployment. Some researchers have developed macro-scale shape memory polymeric composites by reinforcing a shape memory polymeric matrix with fiberglass and Kevlar, and found that the stiffness of SMP increased, whereas the recoverable strain level reduced [14,15]. Cho et al. studied the influence of in situ formed silica by tetraethoxysilane(TEOS) through sol-gel on the shape memory effect and mechanical properties of polyurethane, and found that the mechanical properties were largely influenced by TEOS content, and good shape fixation and shape recovery of more than 80% were obtained for all polyurethane-silica samples [16]. Recently, Gall et al. developed shape memory nanocomposites by introducing nanoscale SiC particulates to shape memory polymeric matrix, and found that the resulted shape memory nanocomposites have a higher elastic modulus and are capable of generating higher recovery force as compared to the pure SNIP resin [17].

In this work, we prepared a series of hybrid polyurethanes (HYPUs) cross-linked by Si–O–Si domains, which may not only act as the net-points for dimension stability but also act as 'inorganic fillers' for reinforcement. The HYPUs were characterized from the aspects of morphology, thermal properties, dynamic mechanical properties and shape memory behaviors. The work will provide a new direction in designing shape memory systems since the shape memory temperature and mechanical properties can be adjusted by the content of Si–O–Si in the composites.

2. Experimental

2.1. Materials

2-Hydroxyethylacrylate (HEA) was obtained as a gift from Taiwan Eternal Chemical Co., China. 3-Aminopropyl triethoxysilane (KH550) is a product of Nanjing Yudeheng Co., China. Both were distilled under N_2 before use. *N*,*N*′-Dimethylacetamide (DMAc) was freshly distilled at the existence of CaH before use. Poly(ethylene glycol). (PEO400 $M_W = 400$ g/mol, Shanghai First Reagent Co., China) was dried under reduced pressure at 120 °C. Isophorone diisocyanate (IPDI) and dibutyltindilaurate (DBTDL), purchased from Aldrich Co., USA and Shanghai First Reagent Co., China, respectively, were used as received.

2.2. Synthesis

The synthesis of hybrid polyurethanes is straightforward as shown in Scheme 1.

2.2.1. Hybrid diol (HD)

HEA (58.06 g, 0.50 mol) was introduced into a 250 ml three-neck flask equipped with a mechanical stirrer, a drop funnel and a N_2 inlet. KH550 (55.34 g, 0.25 mol) was then dropped slowly into the flask below 30 °C. After stirred vigorously under N_2 for 20 h, a viscous transparent fluid was resulted (113.40 g).

2.2.2. Hybrid polyurethane (HYPU)

HYPUs were prepared from PEO400, IPDI and HD at different ratios (Table 1) by a conventional two-step method. Into a 250 ml three-neck flask quipped with a mechanical stirrer and a nitrogen inlet, freshly distilled DMAc, PEO400, IPDI, and DBTDL (0.3% w/w) were introduced. After stirred under N_2 at 80 °C for 4 h, the temperature was decreased to 70 °C. An appropriate amount of HD according to IPDI/(PEO400 + HD) = 1 was added and the reaction proceeded at 70 °C for another 4 h. The resulted viscous mixture was poured into a large amount of ice-cooled ether. After washed for three times with ice-cooled ether, the resin was re-dissolved in DMAc to produce a 30 wt% solution. H_2O and 1.0 M HCl were added at the ratio of H_2O:HCl:Si–OEt = 2:0.018:1 and the solution were stirred at room temperature for 2 h, the resulted

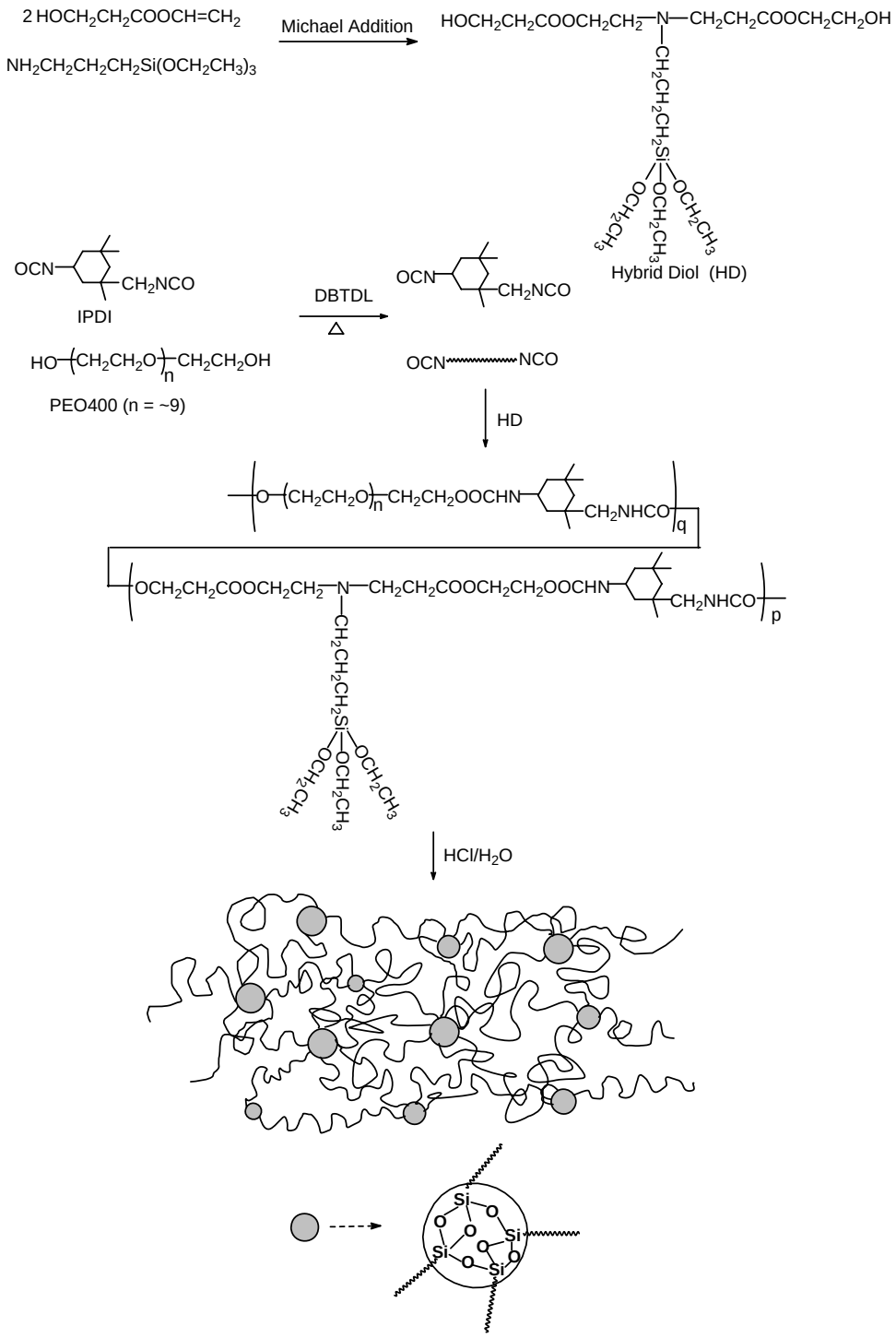

Scheme 1. Outline of preparation process for HYPUs.

sol was then poured into a teflon mold, and kept at 60 °C for 24 h, and 120 °C for another 24 h in a vacuum oven. The obtained films were cut into appropriate shape for tests.

2.3. Measurements

2.3.1. FTIR and NMR

The FTIR spectra were recorded on a Nicolet MAGNA-IR 750 spectrometer. The nuclear magnetic resonance (NMR) measurement was performed on an AVANCE AV 400 instrument (Brucker Co., Switzerland) using $(CD_3)_2CO$ as a solvent and TMS as a reference. The ^{29}Si NMR spectrum was recorded with a 30° pulse width and 15 s recycle delay.

2.3.2. Thermal properties

The thermal properties (glass transition temperature and melting temperature) were measured using a Perkin–Elmer Diamond differential scanning calorimeter (DSC) with

Table 1
Thermal and dynamic mechanical properties of HYPUs

Sample	PEO: HD (mol/mol)	T_g^{DSC} [a] (°C)	T_g^{DMA} [b] (°C)	E'_{low} [c] (MPa)	E'_{high} [d] (MPa)	E'_{low}/E'_{high}	ν_e [e] (mol/L)
HYPU0-1	0:1	53.2	57.0	2250	16.34	144	1.99
HYPU1-4	1:4	34.3	50.5	2140	13.71	170	1.70
HYPU1-2	1:2	27.8	47.5	1885	8.762	272	1.10
HYPU1-1	1:1	19.1	35.9	1540	3.850	786	0.50

[a] Measured from DSC curves.
[b] Measured from the peak tan δ curve.
[c] At the temperature of $T_g^{DMA}-25$ °C.
[d] At the temperature of $T_g^{DMA}+25$ °C.
[e] Calculated from $\nu_e=E'_{high}/3RT_{high}$ ($T_{high}=T_g^{DMA}+25+273$ K).

a heating rate of 10 °C/min from −60 to 140 °C, and then cooled to −60 °C at a cooling rate 200 °C/min, followed by a second scan at the same heating rate to 140 °C. The measured DSC curves were calibrated with baseline. The mid-point of the start and end of the transition in DSC curves was taken as the T_g^{DSC} value.

2.3.3. Wide angle X-ray scattering

Wide angle X-ray scattering (WAXS) analysis was performed with thin film samples of 0.5–1.0 mm thickness using a Rigaku D/max-rA X-ray diffractometer (Rigaku Co., Japan) operated at 40 kV and 100 mA with Cu ($\lambda=1.54178$ Å) irradiation at the rate of 2°/min in the range of 10–60°.

2.3.4. Dynamic mechanical analysis

A Pyris Diamond DMS 6100 instrument (Perkin–Elmer Co., USA) was run in a tensile mode at an oscillation frequency of 1 Hz with a static force of 10 mN and a oscillation amplitude of 10.0 μm (~0.05% strain). The samples of around 20×10×0.8 mm^3 were measured over a temperature range from −60 to 120 °C at a heating rate of 2 °C/min under nitrogen gas purging. The T_g^{DMA} values were taken from the peaks of tan δ curves.

2.3.5. Shape memory behavior

The method of bending test [4] was adopted to evaluate the shape memory properties. HYPU films were cut into rectangular strips with the dimension of 1.0×7.0×32.0 mm^3. The test was carried out as the following procedures: (1) bending the sample to be in a circular shape with an inner diameter of 10.0 mm in 5 s at the deforming temperature (T_{def}, 25 °C higher than its T_g^{DMA}) (T_g^{DMA} in the bending test refers to the value measured from DMA); (2) cooling the sample down to the fixing temperature (T_{fix}, 25 °C lower than its T_g^{DMA}) without releasing the deforming stress; (3) keeping the sample at T_{fix} for 5 min after the removal of the deforming stress, (4) finally, heating the sample up to T_{def} again, the sample shape varied as a function of time. The shape recovery progress was monitored by a Canon PowerShot A70 video camera. The variation of curvature ($k=1/r$, r=radius of circles superposing the curved samples) of the bent samples was plotted against time to compare the shape recovery effect of HYPUs.

3. Results and discussion

3.1. Preparation and characterization

The HD was synthesized from KH550 and HEA through Michael addition, which is a quantitative reaction confirmed by ^{1}H NMR (Fig. 1) and ^{29}Si NMR. All hydrolysable Si–OEt groups remained since the peaks for Si–OEt group are in accordance with its ideal structure and just one signal at −44.7 ppm was observed in ^{29}Si NMR spectrum. The introduction of HD into the main chains of HYPUs resulted in the polyurethanes containing cross-linkable Si–OEt groups, which hydrolyzed and condensed to form networks after adding water under an acid catalyst. It's also observed that the polyurethane prepared just by PEO400 and IPDI under the same condition cannot form dimensional stable films under room temperature, which confirmed that it's the hydrolysis and

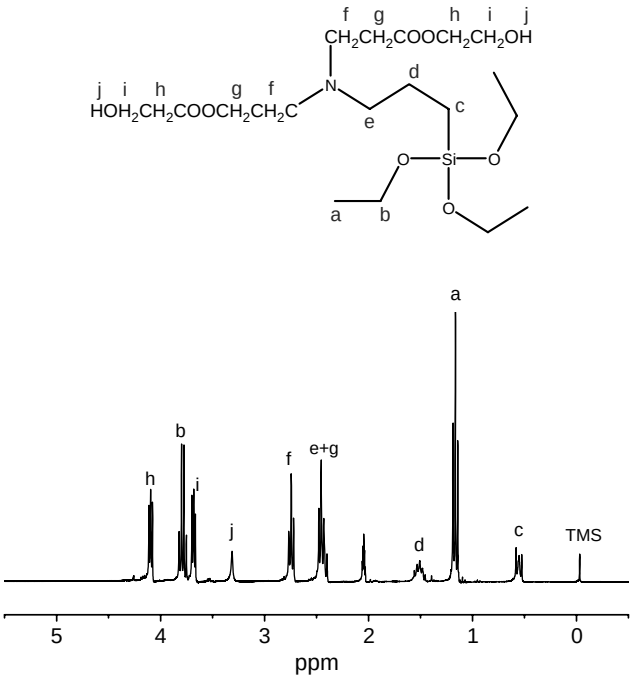

Fig. 1. ^{1}H NMR spectrum of HD.

condensation of Si–OEt that pr ides HYPUs film-forming ability.

3.2. Morphology

To investigate the underlying microstructure of HYPUs cross-linked by Si–O–Si with different content, wide-angle X-ray scattering (WAXS) was employed. As shown in Fig. 2, all samples show similar WAXS curves with a large and a small wide diffraction halo at around 20 and 42° respectively, which are typical for amorphous polymeric materials since the molecular chain distance in non-crystalline materials is about 0.4–0.5 nm. It has been observed that some crystal structures exist in many physical cross-linked polyurethane systems due to the strong hydrogen bonding, dipole–dipole interaction and induced dipole–dipole interaction in the hard segments. In a strict sense, there is no 'hard segment' in the HYPU system since that the chains of PEO400 and HD both are not short or rigid to favor the forming of 'hard segment'. In one hand, the absence of distinct crystalline reflection in the WAXS pattern is ascribed to the lack of 'hard segment'. In another hand, the inorganic Si O Si network also disturbs the orientation of polyurethane molecular chains. As found by Jiang et al. [18] in their work, the movement of PEO chains is highly confined in the PEO/silica organic–inorganic hybrid network, PEO is in amorphous state when the concentration of PEO is lower than 50 wt%. In our work, the concentration of PEO is much lower than 50 wt%, and the chain length of PEO is also not long enough for crystallization orientation.

3.3. Thermal properties

The thermal properties of HYPU networks were characterized with DSC by heating the samples from −60 to 140 °C at 10 °C/min, followed cooling to −60 °C at 200 °C/min and reheating the samples to 140 °C at 10 °C/min. Two heating scans have not show any difference, which further validates the absence of crystalline phase. There is only one glass transition stage in DSC curve for each sample as shown in Fig. 3, indicating the homogeneity of HYPUs. Both of the absence of any melting peak for crystallites and single glass transition temperature can also be anticipated from the optically clear appearance of these materials.

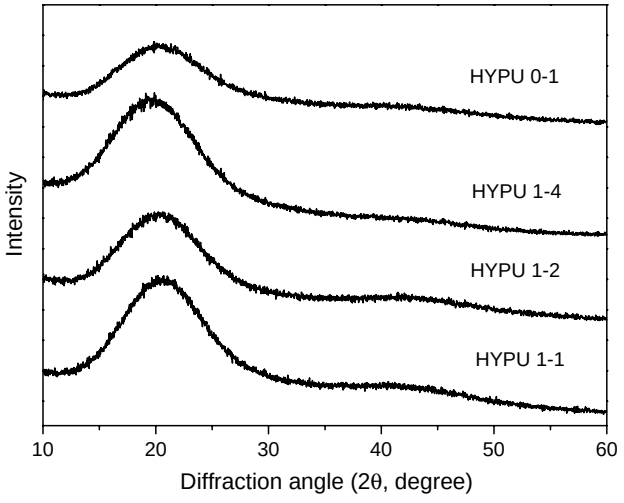

Fig. 2. WAXS measurements for HYPUs.

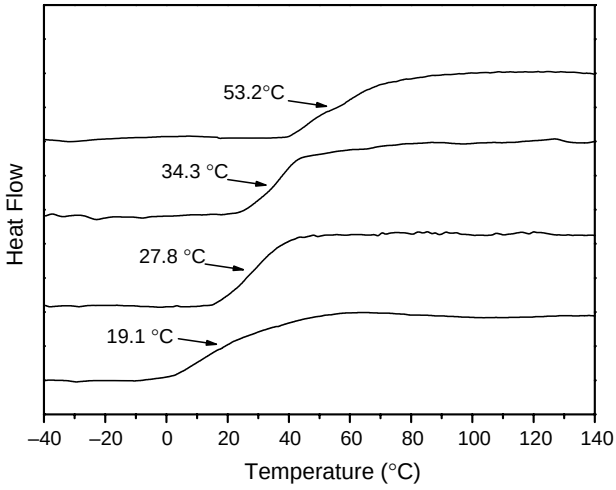

Fig. 3. DSC scans of HYPUs.

The T_g^{DSC} value increases with decreasing the PEO/HD ratio, and reaches to 53.2 °C for the sample HYPU0-1 containing no PEO. The average chain length between the net-points decreased with HD content increasing, so it seems reasonable to assume that the mobility of organic polyurethane chains is greatly restricted by hard inorganic Si–O–Si network. By changing the PEO/HD ratio, materials with different T_g^{DSC} can prepared to satisfy the temperature requisite according to different applications. The T_g^{DSC} values of the prepared samples are in the range of 19–54 °C, falling into the neighborhood of human body temperature, which will give a prospect for such materials to be used as biomedical mechanics in minimally invasive surgery fields.

3.4. Dynamic mechanical behaviors

When subjected to a sinusoidal dynamic stress, a polymeric beam in clamps will exhibit a sinusoidal tension that lags behind the applied stress with a phase angle δ_0. From the relation between stress and strain, the storage modulus E' and the loss modulus E'' can be calculated. The ratio of E''/E' is the loss tangent tan δ, which reflects the viscous-elastic characteristic of a polymeric material. The T_g^{DMA} values of HYPUs are obtained from the peaks of tan δ curves. From the theory of rubber elasticity, the cross-link density (v_e) of a cross-linked polymer can be determined by the following equation:

$$E' = 3v_eRT$$

where E' is the storage modulus of the cross-linked polymer in the rubbery plateau region above T_g (i.e. $T_g^{DMA} + 25$ °C), R is the gas constant (8.314 J K^{-1} mol^{-1}), and T is the absolute temperature (K). The obtained results are summarized in Table 1.

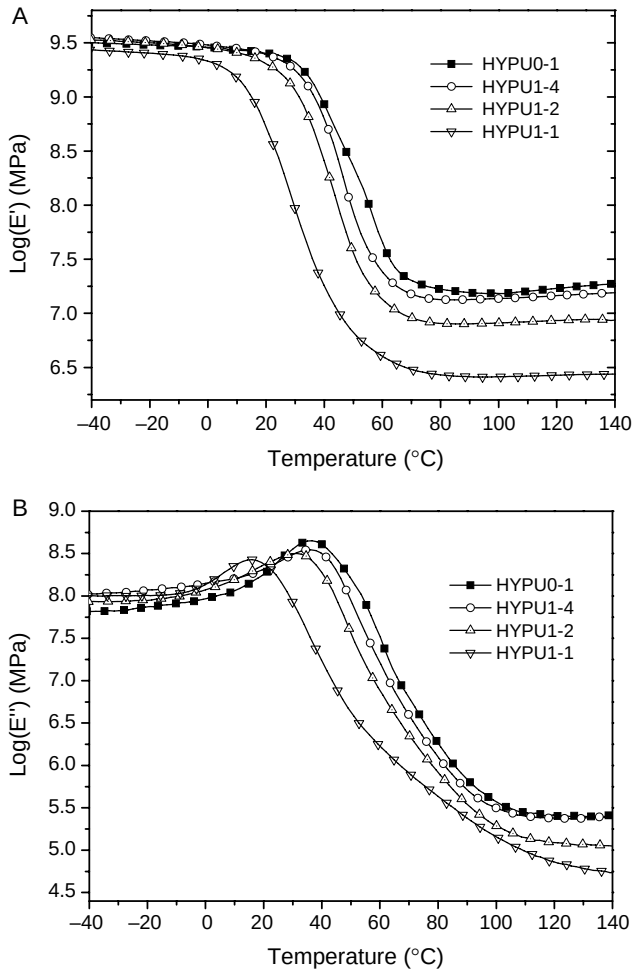

Fig. 4. (A) Logarithm of dynamic storage modulus (E') and (B) logarithm of loss modulus (E'') vs. temperature.

Fig. 4 shows the dynamic storage (or elastic) modulus (E') and loss (or viscous) modulus (E'') as a function of temperature for HYPUs. All materials exhibit the behavior typical of cross-linked polymeric network with respect to E' curves. There are a glass state at low temperatures with E' staying at a high modulus plateau and a rubbery state with a lower E' for a wide range of high temperatures. The storage modulus begins to fall sharply at 0, 13, 23 and 31 °C for HYPU1-1, HYPU1-2, HYPU1-4 and HYPU0-1, respectively. Related with the DSC curves in Fig. 3, the fall of E' in Fig. 4 should be ascribed to the glass transition of amorphous polymeric network. All HYPU samples show high storage modulus ratios beyond 100 ($E'_{low}/E'_{high} > 100$) and high modulus at the scale of 10^6 Pa (Table 1) at high temperature. For shape memory materials, the high ratio of storage modulus below T_g^{DMA} to that above T_g^{DMA} is preferred, which is in favor of the deformation at high temperatures and the fixing of temporary shape at low temperatures. The high modulus at high temperature can result in more stress reservation of deformation during cooling, which will be advantageous for shape recovery. It can be seen from Fig. 4 that HYPUs with a lower PEO/HD ratio show higher storage modulus both in the glass state and rubbery state

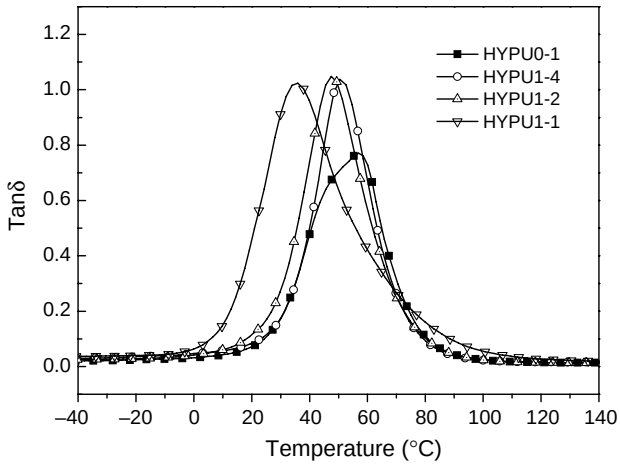

Fig. 5. Tan δ vs. temperature curves.

because that the cross-linking density (v_e) and hard inorganic Si–O–Si reinforcement increased with PEO/HD ratio decreasing. As shown in Table 1. The storage modulus at low temperature (E'_{low}) increased from 1540 MPa for HYPU1-1 to 2250 MPa for HYPU0-1 and the storage modulus at high temperature (E'_{high}) increased from 3.850 MPa for HYPU1-1 to 16.34 MPa for HYPU0-1 when the cross-linking density (v_e) increased from 0.50 mol/L for HYPU1-1 to 1.99 mol/L for HYPU0-1.

Fig. 5 shows the dissipation factor tan δ curves as a function of temperature for HYPUs. The location of tan δ peak is strongly dependent on PEO content which shifts to higher temperatures with PEO/HD ratio decreasing. This can be explained that the cross-linking net-points increased and the average chain length between net-points decreased as more HD are incorporated into polyurethane chains. Consequently, the polyurethane molecular chains are more restricted and higher temperature is needed to activate their local mobility in a lower PEO/HD ratio. The glass transition breadth measured from the tan δ curves show some reduction with the cross-linking density increasing, which is consistent with the transition width shown in DSC measurements (Fig. 3), indicating that HYPUs incorporating more HD in main chains have more homogeneous network structures. The glass transition temperature determined from the peaks of tan δ curves is higher than that determined by DSC as summarized in Table 1, which is related to the heat transporting hysteresis for larger scale samples in DMA, while the DSC transition being measured is more toward smaller scale segmental mobility, which occurs at a lower temperature. The magnitude of tan δ as shown in Fig. 5 is also affected by the HD/PEO ratio. The peak value of tan δ is 0.77 for HYPU0-1 and it is about 1.0 for the other three samples, suggesting that the incorporation of soft PEO chain makes the hybrid urethanes more likely viscous than elastic. Since tan δ value corresponds to the strain energy dissipated by chain friction, the high tan δ value of HYPUs makes them a good candidate for smart fabric materials with damping capability [5].

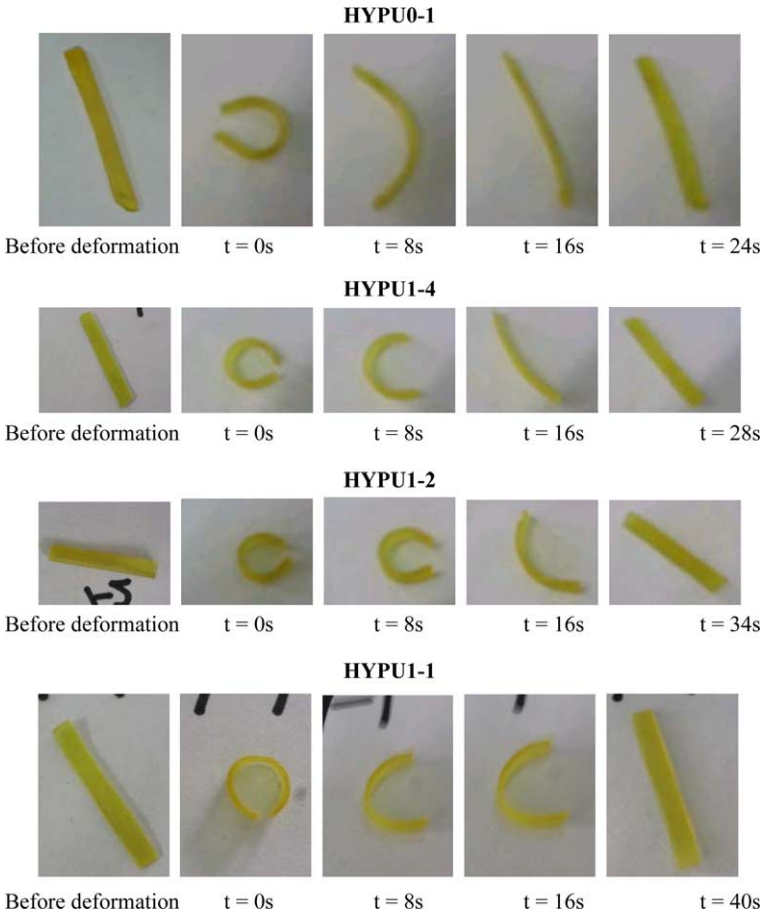

Fig. 6. Shape recovery process for HYPUs.

3.5. Shape memory behaviors

Most of shape memory polymeric elements are practically used in the strain of below 20%. It's also a fact that the bending deformation is widely employed for evaluating shape memory polymeric elements and a large deflection is easily obtained in the range of small strain through bending [19]. Therefore, the bending test was employed here to evaluate the shape fixing and the shape recovery of HYPUs. Fig. 6 shows the shape recovery progress of HYPUs at T_{def}. The pictures at $t=0$ s represent the shapes of bended samples when they were kept at T_{fix} for 5 min after releasing the external stress. All samples show excellent shape fixing with the preservation of circle frames, indicating that the micro-Brownian movements of molecular chains in amorphous networks are frozen at T_{fix}. The rapid shape recovery speed was observed for all samples, which can regain their original shapes with the degree of almost 100% in 40 s at T_{def} in air. To quantitatively evaluate the recovery speed, the time evolution of curvature determined from the images during the recovering process was shown in Fig. 7. It's clear that the shape recovery rate increases with increasing the HD/PEO molar ratio in the hybrid polyurethanes. Comparing the shape recovery extent after the same time (such as the images after 16 s in Fig. 6) shows a straightforward result. Among them, HYPU0-1 shows the lowest shape fixing and the quickest shape recovery rate. Related with the storage modulus and tan δ curves in Figs. 4 and 5, the lower shape fixing and quicker shape recovery speed in samples with higher HD/PEO ratio should ascribe to their higher storage modulus at T_{def} and lower tan δ value. For the samples with higher storage modulus at high temperature, more deforming energy is needed at T_{def} and more energy are stored

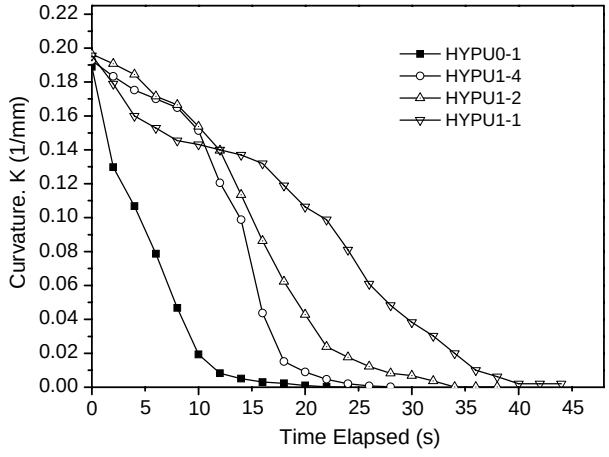

Fig. 7. Time evolution of curvature at T_{def}.

with the loss of elastic entropy when cooling down to T_{fix}. Moreover, the lower tan δ values for samples with higher HD/PEO ratio also indicate that higher percentage of deforming energy are stored than dissipated. As a result, the samples with higher storage modulus at T_{def} and lower tan δ values have higher tendency to return to their original shapes. So, the shape fixing decreases and the shape recovery speed increases with HD/PEO ratio increasing.

For a better understanding of the shape memory mechanism of HYPUs, each sample with the dimension of $1.0\times7.0\times32.0$ mm^3 is bended into a circle at 90 °C in air and then cooled down to 0 °C and kept at 0 °C for 10 min. The shape recovery rates of the samples at different temperatures are monitored with camera after they are kept at the temperature for 5 min. The resulted evolutions of curvature with temperature are shown in Fig. 8. The temperature at which the sharpest transition takes place increases with the samples incorporating more HD and the temperature ranges of the sharp transition are consistent with the T_g^{DMA} values determined from DMA, indicating that the shape recovery is mainly driven by the micro-Brownian movements of molecular chains, which is activated around T_g^{DMA}. The curvature curves in Fig. 8 show more abrupt drops for the samples with lower PEO/HD ratio, namely the samples with more HD have higher tendency to regain their original shape, which is in accord with the result from Fig. 7.

The shape memory behaviors of HYPUs were also studied in water to explore their recovery ability for the potential applications in body. The specimens with a dimension of $1.0\times7.0\times60.0$ mm were coiled into two circles at T_{def} and then cooled down to T_{fix}. It was found that the samples successfully regained their original straight linear shapes in less than 10 s when immersed into hot water at T_{def}. The excellent shape recovery of HYPUs in water indicates that the recovery stress of HYPUs is large enough for some applications with constraint environments. Detailed work about the constrained shape recovery for HYPUs is underway.

An important issue about shape memory materials is about their shape recovery rate change due to repetition. The change of strain fixing and shape recovery rate is usually observed in many physically cross-linked polyurethane systems especially in the first cycles due to the reorganization of molecular chains in the deforming direction [1]. For HYPUs tested in air, no significant change of shape fixing and shape recovery rate due to repetition is observed in the tested cycles (>50). While the shape fixing decreases significantly for the samples tested in water. After the samples tested in water were dried in air, they can regain the original shape memory effect, indicating that the water dissipated into the polymeric matrix has pronounced effect on their micro-structure [20].

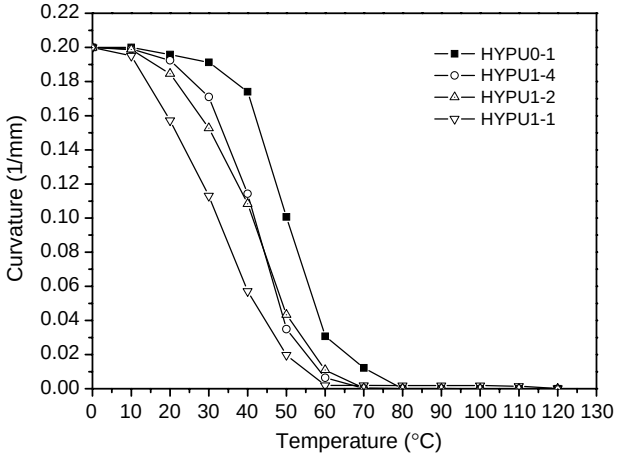

Fig. 8. Recovered curvatures at different temperatures.

4. Conclusions

It's the first synthesis of hybrid polyurethanes cross-linked by Si–O–Si having shape memory effect. The synthetic route to HYPU allows a convenient adjustment of network cross-linking and the resulted thermal and mechanical properties. The morphology and thermal properties studied by WAXS and DSC, respectively, indicated that HYPUs have amorphous cross-linked network structures. The T_g values of HYPUs obtained from DSC and DMA increased with PEO/HD ratio decreasing, indicating that the Si–O–Si linkings formed through hydrolysis and condensation of Si–OEt have pronounced reinforcement effect in restricting the mobility of chains. The sharp storage modulus transition around T_g^{DMA} endues HYPU samples with excellent shape memory properties. The shape memory behaviors indicated that the shape fixing and shape re speed of HYPU samples were dominated by the storage modulus above and below T_g^{DMA}, tan δ value. The samples incorporating more HD have lower shape fixing and faster shape recovery speed. The excellent shape memory behaviors of HYPUs provide them a perspective for the applications in biomechanics.

Acknowledgements

This work has been supported by China NKBRSF Project (No. 2001CB409600) and National Natural Science Foundation of China (50233030).

References

[1] Lendlein A, Kelch S. Angew Chem Int Ed 2002;41(12):2034–57.
[2] Metzger MF, Wilson TS, Schumann D, Matthews DL, Maitland DJ. Biomed Microdevices 2002;4(2):89–96.
[3] Liu GQ, Ding XB, Cao YP, Zheng ZH, Peng YX. Macromolecules 2004; 37(6):2228–32.
[4] Liu CD, Chun SB, Mather PT, Zheng L, Haley EH, Coughlin EB. Macromolecules 2002;35(27):9868–74.
[5] Lee BS, Chun BC, Chung YC, Sul KI, Cho JW. Macromolecules 2001; 34(18):6431–7.
[6] Yang JH, Chun BC, Chung YC, Cho JH. Polymer 2003;44(11): 3251–8.
[7] Kim BK, Shin YJ, Cho SM, Jeong HM. J Polym Sci, Part B: Polym Phys 2000;38(20):2652–7.
[8] Lin JR, Chen LW. J Appl Polym Sci 1998;69(8):1575–86.
[9] Kim BK, Lee SY, Lee JS, Baek SH, Choi YJ, Lee JO, et al. Polymer 1998; 39(13):2803–8.

[10] Jeong HM, Lee JB, Lee SY, Kim BK. J Mater Sci 2000;35(2): 279–83.
[11] Lee SH, Kim JW, Kim BK. Smart Mater Struct 2004;13(6): 1345–50.
[12] Cho JW, Jung YC, Chung YC, Chun BC. J Appl Polym Sci 2004;93(5): 2410–5.
[13] Alteheld A, Teng YK, Kelch S, Lendlein A. Angew Chem Int Ed 2005; 44(8):1188–92.
[14] Liang C, Rogers CA, Malafeew E. J Intell Mater Syst Struct 1997;8(4): 380–6.
[15] Ohki T, Ni QQ, Ohsako N, Iwamoto M. Compos Pt A-Appl Sci Manuf 2004;35(9):1065–73.
[16] Cho JW, Lee SH. Eur Polym J 2004;40(7):1343–8.
[17] Gall K, Dunn ML, Liu YP, Finch D, Lake M, Munshi NA. Acta Mater 2002;50(20):5115–26.
[18] Jiang S, Yu D, Ji X, An L, Jiang B. Polymer 2000;41(6):2041–6.
[19] Tobushi H, Okumura K, Hayashi S, Ito N. Mech Mater 2001;33(10): 545–54.
[20] Yang B, Huang WW, Li C, Lee CM, Li L. Smart Mater Struct 2004;13: 191–5.